Photochemical & Photobiological Sciences

Accepted Manuscript

This is an *Accepted Manuscript*, which has been through the Royal Society of Chemistry peer review process and has been accepted for publication.

Accepted Manuscripts are published online shortly after acceptance, before technical editing, formatting and proof reading. Using this free service, authors can make their results available to the community, in citable form, before we publish the edited article. We will replace this *Accepted Manuscript* with the edited and formatted *Advance Article* as soon as it is available.

You can find more information about *Accepted Manuscripts* in the Information for Authors.

Please note that technical editing may introduce minor changes to the text and/or graphics, which may alter content. The journal's standard Terms & Conditions and the Ethical guidelines still apply. In no event shall the Royal Society of Chemistry be held responsible for any errors or omissions in this *Accepted Manuscript* or any consequences arising from the use of any information it contains.

ROYAL SOCIETY OF CHEMISTRY

www.rsc.org/pps

Photophysical and calorimetric investigation on the structural reorganization of poly(A) by phenothiazinium dyes azure A and azure B

Puja Paul and Gopinatha Suresh Kumar*
Biophysical Chemistry Laboratory, Chemisry Division
CSIR-Indian Institute of Chemical Biology
Kolkata 700 032, India

Address for Correspondence:
Dr. G. Suresh Kumar, Ph.D
Scientist
Biophysical Chemistry Laboratory
CSIR-Indian Institute of Chemical Biology
4, Raja S. C. Mullick Road
Kolkata 700032, INDIA
Phone: +91 33 2472 4049/2499 5723
Fax: +91 33 2473 0284 / 5197
e-mail: gskumar@iicb.res.in/gsk.iicb@gmail.com

*author to whom all correspondence should be addressed.

Highlights

- The binding of AA and AB to ss poly(A) was cooperative in nature.
- The binding resulted in significant perturbation of the poly(A) conformation.
- The binding induced self-structure formation in ss poly(A).
- The binding was exothermic and predominantly entropy driven.
- Heat capacity change and enthalpy-entropy compensation characterized the binding.

Abstract

Poly(A) has significant relevance to mRNA stability, protein synthesis and cancer biology. The ability of two phenothiazinium dyes azure A (AA) and azure B (AB) to bind single-stranded poly(A) was studied by spectroscopic and calorimetric techniques. Strong binding of the dyes and the higher affinity of AA over AB was ascertained from absorbance and fluorescence experiments. Significant perturbation of circular dichroism spectrum of poly(A) in the presence of these molecules with formation of induced CD bands in the 300-700 nm region was observed. Significant emission polarization of the bound dyes and strong energy transfer from the adenine base pairs of poly(A) suggested intercalative binding to poly(A). Intercalative binding was confrimed from fluorescence quenching experiments and was predominantly entropy driven as evidenced from isothermal titration calorimetry data. The negative values of heat capacity indicated involvement of hydrophobic forces and enthalpy-entropy compensation suggested non covalent interactions in the complexation for both dyes. Poly(A) formed self-assembled structure on the binding of both the dyes that was more favored at higher salt conditions. New insights in terms of spectroscopic and thermodynamic aspects into self-structure formation of poly(A) by two new phenothiazinium dyes that may lead to structural and functional damage of mRNA are revealed from these studies.

Keywords: Phenothiazinium dyes; Poly(A); Self-assembly; Spectroscopy; Calorimetry

Introduction

All mRNAs in eukaryotic cells have a poly(A) chain of about 200-250 bases at the 3'-end that confers them the stability and influences the transcription process. Polyadenylation of the mRNAs, catalyzed by the enzyme poly(A) polymerase (PAP), is a critical post transcriptional cellular event resulting in the maturation of all eukaryotic mRNAs before the begining of the translation process. The discovery of Topalian et al that Neo-PAP (a human PAP) is overexpressed in some human cancer cells has fueled speculation that the poly(A) tail of mRNAs may represent a malignancy specific target[1] for anticancer agents. Small molecule therapeutics can interact with poly(A) and degrade poly(A) or induce secondary structural organization, that may resemble the poly(A).poly(A) duplex.[2] The induction of such a structure by small molecules at physicological condition in vivo could prevent the binding of poly(A)-binding protein to its inherent target and hence may be useful as potential lead compounds for controlling the poly(A) chain elongation leading to mRNA degradation and arrest of cell proliferation. Recently many such small molecules that induce self-structure in poly(A) have been discovered and the formation of such structure arose curiosity to understand the molecualr aspects of such reorganization.[3-10]

Azure A (AA) and azure B (AB) are two important dyes with the same basic phenothiazinium skeleton but with different groups at the 7 position (Fig. 1). These compounds have been recently employed in a number of biological and chemical studies such as evaluations focused on the biochemical mechanisms of Alzheimer disease.[11] They are also used as a model for phototherapeutic agents as well as for dye sensitized solar energy conversion.[12-13] These phenothiazinium dyes are known to localize in the plasma membrane of yeasts. Due to the increased permeability of the dyes, the cellular structure is damaged upon illumination

resulting in cell death.[14-15] The azure dyes can interfere through fluorescent radiation absorption that is emitted by excited molecules, resulting in a photobactericidal effect on the *Staphylococcus aureus* and *Enterococcus faecium* colonies.[13]

Azure A, asymmetrical dimethylthionine, has found wide industrial applications as electrochromic devices, solar energy cells and optical sensors.[16] Kean[17] reported a rapid nonhydrolytic method for the quantitative estimation of sulfatide, a well known component of mammalian tissue using this dye. An ion-pair extraction technique with azure A solution was used for differentiating biles of normal subjects and patients with liver disease from patients with Crohn's disease.[18] Recently, AA has been employed to ascertain presence of anionic detergents in milk.[19]

Azure B, monodemethyl methylene blue, is easily available phenothiazinium dye and has been widely employed both in metal determination and DNA staining detection.[20] AB, given intravenously to BCG-sensitized mice 15 minutes prior to challenge with lipopolysaccharide, prevented death from endotoxic shock.[21] It was also capable of decreasing the blood serum level of tumor necrosis factor alpha by a factor of 10. It is a better inhibitor of human glutathione reductase and related enzymes compared to methylene blue.[22] A facile and sensitive method for the determination of trace amounts of vanadium[23] and selenium[24], both of which are toxic environmental pollutants using AB as a chromogenic reagent was developed. Recently, azure B has been found to be a potent monoamine oxidase A (MAO-A) inhibitor (IC_{50} = 11 nM), approximately 6-fold more potent than methylene blue (IC_{50} = 70 nM) under identical conditions. AB also reversibly inhibits the MAO-B isozyme with an IC_{50} value of 968 nM. Results suggested that AB may be a hitherto under recognized contributor to the

pharmacology and toxicology of methylene blue by blocking central and peripheral MAO-A activity.[25]

Our long-term interest in developing antitumor agents derived from different sources prompted us to investigate the potential of these DNA-binding dyes to specifically target poly(A) sequences and induce a self-structure formation. The present study is devoted to elucidation of the molecular details of the binding process of dye-poly(A) complexation through multifaceted biophysical experiments.

Results and discussion

Spectrophotometric studies

The binding of the dyes to poly(A) was followed by means of absorption titration in the 450-700 nm (Fig. 2a,b). Poly(A) has no absorption in this region. Fig. S1 shows characteristic UV-visible absorption spectrum of AA and AB in aqueous buffer of pH 7.2. The spectra exhibited three well-resolved maxima at 245, 289 and 633 nms for AA and 245, 290 and 642 nms for AB. The maximum absorbance of AA and AB located around 633 nm and 642 nm, respectively, on titration with increasing concentrations of poly(A) showed hypochromic effect, suggestive of strong intermolecular interaction involving effective overlap of the π electron cloud of the dyes with those of the adenine bases. In the case of AA, flattening of the 633 nm peak occurred while the 598 nm hump of AB became prominent as a result of the interaction. Sharp isosbestic points at 577 nm and 573 nm, respectively, for AA and AB were evidenced. This behaviour was quite different from what was observed upon association of the dyes with DNA.[26] The isosbestic points enabled the assumption of a two state system consisting of bound and free dye at any particular wavelength. The concnetration of the free and bound dyes to poly(A), evaluated from the titration of a constant concentration of poly(A)

with increasing concentration of the dyes, enabled the construction of Scatchard plots of r/C_f versus r to quantify the binding reaction (inset of Fig. 2a,b). Cooperative binding isotherms observed were analyzed further by the McGhee-von Hippel methodology[27] using equation (2) for the evaluation of the binding constants. The cooperative binding affinity (K) values for AA and AB -poly(A) complexation were evaluated to be 1.02×10^5 M^{-1} and 1.17×10^5 M^{-1}, respectively. The apparent binding constants (K_i), the product of K and the cooperative factor (ω), yielded values of 3.06×10^6 M^{-1} and 1.65×10^6 M^{-1}, respectively, for AA and AB. These values are depicted in Table 1.

Fluorescence titration studies

The change in the emission spectra of AA and AB with maxima around 645 and 662 nm when excited at 632 nm and 648 nm, respectively, was monitored by titration with poly(A). Progressive quenching of the fluorescence of the dyes was observed eventually reaching a saturation point without any shift in the wavelength maximum (Fig. 2 c,d). Fluorescence quenching was more (60%) in case of AA-poly(A) complex compared to AB- poly(A) complex (51%).

From fluorescence titration data values close to those obtained from spectrophotometric analysis were obtained by Scatchard analysis (inset of Fig. 2 c,d). The cooperative binding affinity (K) values of AA and AB to poly(A) were evaluated to be 0.51×10^5 M^{-1} and 0.72×10^5 M^{-1}, respectively. The $K_i\omega$ values (Table 1) were 2.96×10^6 M^{-1} and 0.94×10^6 M^{-1}, respectively, for AA and AB. The binding constant of AA was higher than that of the AB in agreement with the results of the absorbption data analysis.

Fluorescence quenching studies by ferrocyanide ions

Fluorescence quenching experiments with anionic quencher like $[Fe(CN)_6]^{4-}$ is an effective method for revealing the accessibility of quenchers to nucleic acid bound samll molecules[4,28] Stern-Volmer plots for the quenching of AA and AB fluorescence complexed with poly(A) are shown in Fig. S3. The K_{sv} values for free AA and its complex with poly(A) were 39 and 8.4 M^{-1}, respectively, and the same for AB were 43 and 14 M^{-1}. This indicated that the bound AA molecules were less accessible to the quencher or in other words bound dye molecules are considerably protected and sequestered away from the solvent suggesting strong binding with poly(A). Thus, ferrocyanide ion quenching results provide direct evidence that the bound AA and AB molecules are truly intercalated. The result also suggest stronger intercalation of AA over AB based on the bulk of the molecules.

Steady-state fluorescence anisotropy

The emission of small molecules is weakly polarized due to their rapid tumbling motion in aqueous media. But on intercalation their rotational motion is restricted and the fluorescence polarization is enhanced. This finding can suggest the probable location of the molecule in heterogeneous environment of poly(A). Fig. 3 shows the variation of fluorescence anisotropy At saturating P/D values, steady-state anisotropy (A) values for azure A and azure B were 0.179 and 0.162, against a value of 0.038 and 0.025 for the free dyes, respectively. The rise in case of AB was steeper compared to AA. These data provide a further support towards probable association of the dyes to poly(A).

Energy transfer from adenine bases of poly(A) to bound dye molecules

The possibility of excited state energy transfer from the poly(A) bases to the bound dye molecules (Fig. 4a) was explored by measuring the excitation spectra of the dyes in the 210-

310 nm region keeping the emission wavelength fixed at 645 nm and 662 nm, respectively, for AA and AB. The light absorption of the dyes in this region is minimum, while poly(A) has strong absorption band around 260 nm. The ratio of the excitation spectra of complex to that of free AA is presented in Fig. 4b. This plot indicates direct emission from the dye and the ratio larger than 1.0 indicates sensitization by poly(A). The band around 290 nm in the excitation spectrum near the region of absorption of poly(A) suggests energy transfer from adenine bases to the dyes. The energy transfer was further confirmed from sensitized emission[29] of the complex which is much more intense than direct emission of the dyes (Fig. 4c).

Fluorescence energy transfer from the bases to the bound dye molecules is manifested by an increase in the quantum yield of bound molecules in the wavelength range of poly(A) absorption. Since energy transfer occurs either due to close contact or through Forster mechanism, the former being more appropriate here, it may confirm both strong binding as well as intercalative mode of binding. Fig. 4d show plots of the ratio Q_λ/Q_{310} against wavelength showing an increase in quantum yield in the region of poly(A) absorbance. The increase in the quantum yield in the poly(A) absorption region suggests energy transfer from the bases to the bound dye molecules that confirms strong intercalative binding. Excitation spectra of the dyes and poly(A) complexes recorded keeping the emission maxima at 645 nm for AA and 662 nm for AB are shown in Fig. 4e and Fig. 4f.

Spectroscopic study using circular dichroism

The characteristic circular dichroism (CD) spectrum of the ss poly(A) was remarkably perturbed in the presence of the dyes (Fig. 5 a,b) resulting in rapid decrease of the 265 and 220 nm positive bands. The change in the 248 nm negative band was not very high. Since the dyes

are optically inactive and do not have any CD signal in the above region, the observed change may be ascribed to that arose in the poly(A) molecule due to the interaction phenomenon. Very often in double stranded DNA, structural change from A-form to B-form and from B-form to C-form results in such large decrease in the long wavelength band ellipticity.[5] Thus it is reasonable to infer that the A-form CD spectrum of poly(A) undergoes structural change to more organized self-structure formation. The change was higher for AA compared to that for AB.

Concomitant with the changes in the intrinsic CD spectra in the UV region, there appeared induced CD spectrum in the 300-700 nm region for the bound dye molecules, the ellipticity of which increased as the binding progressed. Induced CD experiments were performed by keeping a fixed concentration of the dyes (25 μM) with increasing concentration of poly(A). As mentioned above the dyes are optically inactive compound with no intrinsic CD spectrum but acquired induced CD due to their strong association on the helical organization of poly(A). A single negative induced CD band at 566 nm was developed in both the cases. Considering the nature of the induced CD, the intercalated aromatic ring of the dyes appear most likely to be oriented parallel to the adenine bases of poly(A).[30] The presence of an induced CD band in the visible absorption region on complexation with poly(A) further indicates large asymmetry in the environment of the bound molecules inside the poly(A) helix resulting from a strong interaction of the transition moments of the bound molecule with those of the base/base pairs. Based on the strength of the bands, the intercalation of AA appears to be stronger than to AB and is in agreement with the results of other spectroscopic experiments.

Self-assembled structure formation in poly(A)

Due to the critical relevance of poly(A) to mRNA stability, protein synthesis, and cancer biology, we chose to assess the ability of AA and AB to induce single-stranded poly(A) to self structure which has been a recent topic of interest.[2,4,5-6,31-32] Circular dichroism and optical melting experiments of poly(A) in the presence of the two dyes were performed to ascertain the capability of the dyes to induce self-structure formation. Both the dyes induce a stable secondary structure ($T_m \sim 60^oC$), even though this RNA homopolynucleotide is single-stranded in the absence of the dyes. We found cooperative melting of poly(A)-AA and poly(A)-AB complex in optical melting (Fig. 6a) and CD melting (Fig. 6b) profiles at 257 nm clearly confirming the formation of self assembled structure in poly(A) as observed for many alkaloids and planar molecules.[2,4-8]

The DSC melting profiles (C_p versus T) presented in Fig. 6c and 6d further confirmed the induction of self-structure in poly(A) on binding of the two dyes. The DSC melting of poly(A) in the absence of the dyes was a flat thermogram (curve 1, Fig. 6c,d). On the other hand, in the presence of the dyes, the stability of poly(A) enhanced considerably with a melting temperature (T_m) of 59.0±1°C (Fig. 7c and 7d) and the enthalpy of helix denaturation was quite high proving unequivocal evidence for the formation of a self-assembled duplex structure. Again, identical values of vant' Hoff and calorimetric enthalpy (~11.43 kcal/mole) evaluated from the DSC data suggested a truly cooperative reversible transition for the dye bound poly(A) structure. The ratio of the calorimetric enthalpy to vant' Hoff enthalpy is unity indicating cooperative two state transition; that is, the transition occur in an all or none fashion without any intermediate state for the melting of the self-structure of dye- poly(A) complex in complete agreement with the CD and UV melting results. Thus, the planarity in the structure of the dye

moleucles and cooperativity in the binding appears to have a direct correlation to self-structure formation in poly(A), a notion that was proposed from our earlier reports.[4-5,7]

Thermodynamic characterization of the dye-poly(A) interaction

In ITC experiments AA (370 μM) and AB (450 μM) samples were titrated into ss poly(A) solution (20 μM) at 20°C. Fig. 7 a,b (upper panels) shows the representative raw ITC profiles. In the Fig. 7 c,d (lower panels), the corrected injection heats after subtracting control heats are plotted against the respective molar ratios. The data points represent the experimental injection heats and the solid lines denote the calculated fits of the data. The binding affinity and the thermodynamic parameters of the complexation are presented in Table 2. The binding affinity values evaluated from the ITC data are in good agreement with those evaluated from the spectroscopic data (Table 1). The result underscores the observation above that AA has a greater affinity towards poly(A) than AB.

Temperature dependent ITC experiments were performed at four different temperatures viz. 10, 15, 20 and 30°C, respectively, for the binding of these dyes with poly(A). The ITC thermograms indicated one binding event at all the temperatures for both dyes. From the variation of ΔH^o with temperature (Fig. S4) the ΔC_p^o values of (-142.23±0.04) cal/mole.K and (-124.34±0.01) cal/mole.K for AA and AB were obtained (Table 2). Negative heat capacity values have been observed for a variety of small molecules and dyes binding to DNA and RNA structures.[28,33-38] A negative ΔC_p^o value is usually associated with changes in hydrophobic or polar group hydration in the free and the complexed molecules and to a lesser extent from changes in molecular vibrations,[39] and considered as an indicator of a dominant hydrophobic effect in the binding process. Although a number of factors can influence the heat capacity change on complex formation, change in solvent accessible surface area has been shown to be

large component of ΔC_p^o.[40-41] Furthermore, several other molecular contributions for heat capacity changes like change in conformation of poly(A), restriction of the vibrational modes of the bound dye molecule on complexation are likely. The significant differences in the ΔC_p^o values may indicate differences in the role of these forces in each system and also reflect the differences in the amount of structured water released consequent to the transfer of non-polar groups to the inside of the poly(A) helix. Slightly higher ΔC_p^o values of AA compared to AB may also suggest conformational differences in the complex structure and also differences in the disruption of the water structure around adenine bases on complexation. DNA recognition by small molecules have been classified as sequence specific, nonspecific, minimal sequence specific or structure specific.[42] Small negative ΔC_p^o values is generally considered to be the hallmark of minimal sequence specific binding. The slightly negative and non-zero ΔC_p^o values observed here appears to denote structure specific binding. The standard Gibbs energy contribution from the hydrophobic transfer step of binding of these molecules may be calculated from the relationship[43]

$$\Delta G_{hyd}^o = 80(\pm 10)\ \Delta C_p^o \qquad (1)$$

The ΔG_{hyd}^o values for AA and AB binding to poly(A) were calculated to be (-11.37±0.04) and (-9.95±0.01) kcal/mole (Table 2). These values are well within the range that was observed for typical DNA and RNA intercalating molecules.[10,33-35,37,44-45]

Enthalpy–entropy compensation

A significant feature observed in the thermodynamics of dye-poly(A) interactions is the general thermodynamic effect termed as the enthalpy-entropy compensation (EEC) phenomenon. Such phenomena may reflect a multiplicity of weak interactions.[44] The thermodynamic data indicated that the binding enthalpy increased and the entropy term $T\Delta S^o$ decreased with

temperature. Interestingly, the standard molar Gibbs energy exhibited only small changes indicating to be independent of temperature in both cases (Table 2) due to the compensating effects of the enthalpy and entropy change, both of which were strong functions of temperature. Fig. S5 depicts the variations of ΔG^o and ΔH^o as a function of $T\Delta S^o$ for poly(A) binding to the two dyes. Linear variation of ΔH^o with $T\Delta S^o$ with slope near unity (0.92 for AA and and 0.88 for AB) is an indication of a more or less complete compensation and this occurs in systems with ΔC_p^o not equal to zero and $\Delta C_p^o > \Delta S^o$. Enthalpy-entropy compensation is often linked to the solvent reorganization accompanying binding interactions.[46] Starikov and Norden correlated the EEC behaviour observed in biomolecular interactions to Carnot-cycle characteristics.[47]

Role of electrostatic interactions: CD and ITC studies

The dyes are positively charged and hence it is reasonable to assume that electrostatic attraction between the positive charge on the dyes and the negative charge on the phosphate group of poly(A) contributes significantly to the observed high affinity between the partners. To ascertain the contribution of electrostatic interaction in the binding process, salt dependent studies were performed by CD and ITC experiments. CD study was done at two other [Na^+] viz. 10 and 200 mM in addition to those performed at 50 mM. As the salt concentration increased, the perturbation of poly(A) structure became more pronounced followed by the higher intensity for the induced CD bands in presence of AA (Fig. S6) and AB (Fig. not shown). It is pertinent to observe that the the induced CD pattern changes from a simple single band at low salt to an exciton split type at 200 nm (inset of Fig. S6) due to the stronger and closer binding of the dye molecules leading to better interaction of the transition moments of the dye and poly(A) base pairs.

The thermodynamic parameters of the binding of the two dyes to poly(A) at four [Na^+] viz. 10, 50, 100 and 200 mM were evaluated from ITC experiments and the results are collated in Table 3. The binding constant moderately increased as the salt concentration increased in the range 10-50 mM and rose remarkably in the range 50-100 and 100-200 mM. Earlier studies on the interaction of the dyes with DNA have reported that as the salt concentration increased the binding affinity decreased due to the shielding of the electrostatic charges.[26]

In our case with increase in [Na^+], shielding of the electrostatic charges in poly(A) might favor the self-assembled structure and increase the binding affinity due to favorable intercalation on to the duplex poly(A). An increase in the binding affinity of methylene blue with increase of salt concentration was previously reported due to the ease of formation of self-assembled structure.[4]

Conclusions

This study has demonstrated that the phenothiazinium dyes AA and AB strongly bound by intercalation to ss poly(A) molecules. The binding resulted in remarkable conformational changes in poly(A) with concomitant generation of optical activity in the bound dye molecules that appear to assume a helical arrangement on binding to poly(A). Energy transfer from the adenine bases to the intercalated dye molecules was also revealed from fluorescence polarization and efficiency studies. The negative enthalpy and positive entropy changes characterize the binding process and both favors the tight binding of the dyes at the interaction site. The binding leads to self-structure formation as evidenced from cooperative circular dichroism and absorbance melting, and differential scanning calorimetry results. Thes results also confirm that AA is a stronger poly(A) binder than AB. The presence of dimethylamine group at position 7 on the phenothiazinium moiety most likely accounts for the reduced

binding in the case of AB. As ss poly(A) plays significant role in eukaryotic cellular processes, these results suggest a potential mechanism by which the dyes can inhibit the process of gene expression and gene transcription leading to its usefulness as a therapeutic agent for arresting cell proliferation. The specific poly(A) binding features of AA and AB revealed here would not only render further opportunity for developing RNA based therapeutic compounds but will also be of great importance in their toxicological evaluation at the molecular level.

Materials and methods

Materials

Polyriboadenylic acid [poly(A)] as potassium salt was purchased from Sigma-Aldrich Corporation (St. Louis, MO, USA) and used without further purification. It was dissolved in the experimental buffer and dialysed at 5^{o}C against the experimental buffer. Concentration of poly(A) in terms of nucleotide phosphate (hereafter nucleotide) was determined as reported.[48,49] AA and AB (dyes in general) were products of Sigma-Aldrich and were recrystallised. The concentrations were determined by absorbance measurement using molar absorption coefficients (ε) as follows: AA- 57,500 M^{-1} cm^{-1} at 633 nm and AB- 43,000 M^{-1} cm^{-1} at 642 nm. All other materials and chemicals were of analytical grade. All experiments were conducted in filtered 50 mM sodium cacodylate buffer, pH 7.2 prepared in deionized and double distilled water.

Preparation of dye solutions

AA (CAS No. 531-53-3, Color Index Number: 52005, purity ~ 80%) and AB (CAS No. 531-55-5, Color Index Number: 52010, purity ~ 89%) (dyes hereafter in general) solutions were freshly prepared each day in the experimental buffer and kept protected in the dark to prevent any light induced photochemical changes. AA and AB were purified over a silica gel column

using chloroform-methanol mixture as elutent. Azure A was extracted with a 7:3 solvent mixture while azure B was eluted by a less polar solvent mixture. Finally, they were re-crystallised and dried under vacuum at room temperature. The purity of the dye samples was then checked by TLC and found to be satisfactory.[50] The overall concentration of the dyes in each experiment was kept at the lowest possible to prevent aggregate formation and adsorption to the cuvette walls. No deviation from Beer's law was observed in the concentration range used in this study.

Absorption and fluorescence spectral studies and evaluation of the binding parameters

Absorbance studies were done on a Jasco V 660 spectrophotometer (Jasco International Co. Ltd., Hachioji, Japan) at 20°C equipped with a thermoelectrically controlled cuvette holder and temperature controller. Matched quartz cuvettes of 1 cm path length (Hellma, Germany) were used. Standard drug-nucleic acid titration methodologies, described in details earlier, were followed.[5,29] Steady state fluorescence measurements were performed on a Shimadzu RF-5301PC spectrofluorophotometer (Shimadzu Corporation, Kyoto, Japan) in 1 cm path length fluorescence free quartz cuvettes.[51] To avoid inner filter effects, the sample absorbance measured at the excitation wavelength was kept below 0.05 absorbance. The concentrations of AA and AB thus were kept at 0.7 μM and 1.14 μM, respectively. The excitation wavelength for AA and AB were 632 nm and 648 nm, respectively, and the emission intensity was monitored in the range 600-700 nm keeping an excitation and emission band pass of 5 nm. A 5 min. equilibration time after each addition of aliquots of ss poly(A) solution into the dye solution was allowed.

The Scatchard isotherms with positive slope at low r values were analyzed using the following McGhee-von Hippel equation for cooperative binding.[27]

$$\frac{r}{C_f} = K_i(1-nr)\times\left(\frac{(2\omega+1)(1-nr)+(r-R)}{2(\omega-1)(1-nr)}\right)^{(n-1)}\left(\frac{1-(n+1)r+R}{2(1-nr)}\right)^{2} \qquad (2)$$

where,

$$R = \{[1-(n+1)r]^2 + 4\omega r(1-nr)\}^{\frac{1}{2}}$$

where K_i is the intrinsic binding constant to an isolated binding site, 'n' is the number of base pairs excluded by the binding of a single dye molecule and ω is the cooperativity factor. All the binding data were analyzed using Origin 7.0 software (Microcal Inc., Northampton, MA, USA) to determine the best-fit parameters of K_i and 'n' to equation (2).

Determination of the binding stoichiometry

The fluorescence signal was recorded for mixture of solutions where the concentrations of both ss poly(A) and the dyes were varied keeping the sum of their concentration constant.[52 -54] The difference in fluorescence intensity (ΔF) of the dyes in the absence and presence of the ss poly(A) was plotted as a function of the input mole fraction of the dyes. The stoichiometry in terms of ss poly(A)-dye $[(1-\chi_{dye})/\chi_{dye}]$ was obtained from the break points where χ_{dye} denotes the mole fraction of the respective dye. The results presented are average of three experiments.

Fluorescence quenching studies

Quenching studies were carried out with the anionic quenchers $[Fe(CN)_6]^{4-}$ as described previously.[33] The data were plotted as Stern-Volmer plots of relative fluorescence intensity (F_o/F) versus $[Fe(CN)_6]^{4-}$.

Fluorescence polarization studies

Fluorescence polarization measurements of AA and AB complexes poly(A) were carried out as per Larsson and colleagues[55] on the Hitachi F4010 spectrofluorimeter as described previously.[51] AA and AB were excited at 632 nm and 648 nm, respectively, and fluorescence signal was monitored at 645 nm and 662 nm, respectively. The excitation and emission slit widths were fixed at 5 nm. Readings were observed 5 minutes after each addition to ensure stable complex

formation. Each reading was an average of four measurements. Steady state polarization anisotropy 'A' is defined as

$$A = (I_{vv} - I_{vh}\, G) / (I_{vv} + 2\, I_{vh}\, G) \qquad (3)$$

where G is the ratio I_{hv}/I_{hh} used for instrumental correction. I_{vv}, I_{vh}, I_{hv} and I_{hh} represent the fluorescence signal for excitation and emission with the polarizer positions set at (0º, 0º), (0º, 90º), (90º, 0º) and (90º, 90º), respectively.

Sensitized emission, fluorescence energy transfer and quantum efficiency determination

Energy transfer from the base to the bound dye molecules was measured from the excitation spectra of the poly(A)-dye complexes in the wavelength range 220-310 nm.[29,56-57] This was verified further by sensitized emission spectra in the 620-720 nm.[56-57] Excitation spectra were recorded keeping the emission wavelength at 645 nm and 662 nm, respectively, for AA and AB. The ratio $Q = q_b/q_f$, where q_b and q_f are the quantum efficiencies of bound and free dye, respectively, was calculated for each wavelength using the equation $Q = q_b / q_f = I_b\varepsilon_f / I_f\varepsilon_b$, where I_b and I_f are the fluorescence intensities in the presence and absence of the poly(A), respectively, and ε_b and ε_f are the corresponding molar extinction coefficients of the dye. A plot of the ratio of Q_λ/Q_{310} against wavelength was made. Since poly(A) has very little absorbance at 310 nm this was chosen as the normalization wavelength.

Spectropolarimetric studies

Circular dichroism (CD) spectra were acquired on a Jasco J815 unit (Jasco International Co. Ltd., Japan) equipped with a Jasco temperature controller (PFD 425L/15) as reported.[5,29] The molar ellipticity values [θ] are expressed in terms of either per nucleotide phosphate (210-400 nm) or per bound dye (300-700 nm).

CD melting profiles were obtained by heating the sample (60 µM of poly(A) and 24 µM of AA or AB) at a scan rate of 0.8°C/minutes and monitoring the CD signal at 257 nm. For the melting profiles, the ellipticity values are expressed in units of milli degrees.

Optical thermal melting studies

Absorbance versus temperature profiles (optical melting curves) of the complexes were measured on a Shimadzu Pharmaspec 1700 unit equipped with a Peltier controlled TMSPC-8 model microcell accessory (Shimadzu Corporation, Kyoto, Japan) as reported previously.[58,59]

Isothermal titration calorimetry

A MicroCal VP-ITC unit (MicroCal, Inc., Northampton, MA, USA) was used for ITC experiments. Protocols described in details previously[5,59] were used for the titrations. The samples for ITC experiments were degassed on the MicroCal's Thermovac unit to prevent air bubble formation in the calorimeter cell. Programmed injection of aliquots of the dye solution from the rotating syringe (290 rpm) into the isothermal chamber containing the poly(A) solution (1.4235 mL) was done by PC controlled software. Appropriate control experiments to determine the heat of dilution of the dyes were performed. The dilution of the dyes was not found to generate any heat. The area under each heat burst curve was determined by integration using the Origin 7.0 software to give the measure of the heat associated with the injection. The heat associated with each dye-buffer mixing was subtracted from the corresponding heat of ss poly(A)-dye reaction to give the heat of dye-ss poly(A) binding. The heat of dilution of injecting the buffer into the poly(A) solution alone was found to be negligible. The resulting corrected injection heats were plotted as a function of molar ratio. A model for one set of binding sites provided the binding affinity (K_a), the binding stoichiometry (N) and the standard molar enthalpy of binding (ΔH^o). The standard molar Gibbs energy change (ΔG^o) and the

standard molar entropic contribution to the binding ($T\Delta S^o$) were subsequently calculated from standard relationships.[59-60] The ITC unit was periodically calibrated and verified with water-water dilution experiments as per the criteria of the manufacturer.

Differential scanning calorimetry

The excess heat capacities as a function of temperature were measured on a Microcal VP-differential scanning calorimeter (DSC) (MicroCal, Inc.,) as described previously.[5,7] At first the sample and reference cells were filled with the buffer solution, equilibrated at 20^{o}C for 15 minutes and scanned from 20^o to 100^{o}C at 50^{o}C/hour. This was repeated to obtain a stable base line. Once a reproducible base line was achieved the sample cell was rinsed and loaded with poly(A) solution and then with dye-poly(A) complexes of different molar ratios and scanned. Each experiment was repeated twice with separate fillings. The thermograms were analyzed to determine the calorimetric transition enthalpy (ΔH_{cal}) as described earlier.[4,5] The temperature at which excess heat capacity is maximum gave the transition temperature (T_m). The calorimetrically determined enthalpy is model-independent and unrelated to the nature of the thermal transition. The model-dependent van't Hoff enthalpy (ΔH_v) was obtained by shape analysis of the calorimetric data. The cooperativity factor was obtained from the ratio ($\Delta H_{cal}/\Delta H_v$).

Acknowledgements

The authors gratefully acknowledge the financial support for this work from the Council of Scientific and Industrial Research (CSIR), Government of India, network project "GenCODE" (BSC0123). Dr. Puja Paul is a NET-Senior Research Fellow of the CSIR. Authors thank all the colleagues of the Biophysical Chemistry Laboratory for their help and cooperation at every stage of this investigation.

Supplementary data

Supplementary data associated with this article can be found, in the online version, at …..

References

1 S. L. Topalian, S. Kaneko, M. I. Gonzales, G. Bond, Y. Ward and J. Manley, Identification and functional characterization of neo-poly(A) polymerase, an RNA processing enzyme overexpressed in human tumors, *Mol. Cell. Biol.*, 2001, **21**, 5614-5623.

2 H. Xi, D. Gray, S. Kumar and D. P. Arya, Molecular recognition of single-stranded RNA: neomycin binding to poly(A), *FEBS Lett.*, **2009**, 583, 2269-2275.

3 P. Giri, M. Hossain and G.Suresh Kumar, RNA specific molecules: cytotoxic plant alkaloid palmatine binds strongly to poly(A), *Bioorg. Med. Chem. Lett.*, **2006**, 16, 2364-2368.

4 M. Hossain, A. Kabir and G.Suresh Kumar, Binding of the phenothiazinium dye methylene blue with single stranded polyriboadenylic acid, *Dyes Pigments*, 2012, **92**, 1376-1383.

5 P. Giri and G.Suresh Kumar, Self-structure induction in single stranded poly(A) by small molecules: studies on DNA intercalators, partial intercalators and groove binding molecules, *Arch. Biochem. Biophys*., 2008, **474**, 183-192.

6 F. Xing, G. Song, J. Ren, J. B. Chaires and X. Qu, Molecular recognition of nucleic acids: coralyne binds strongly to poly(A), *FEBS Lett*., 2005, **579**, 5035-5039.

7 P. Giri and G.Suresh Kumar, Specific binding and self-structure induction to poly(A) by the cytotoxic plant alkaloid sanguinarine, *Biochim. Biophys. Acta*, 2007, **1770**, 1419-1426.

8 P. Giri and G. Suresh Kumar, Molecular recognition of poly(A) targeting by protoberberine alkaloids: in vitro biophysical studies and biological perspectives, *Mol. Biosyst*., 2010, **6**, 81-88.

9 M. M. Islam, A. Basu and G. Suresh Kumar, Binding of 9-O-(ω-amino) alkyl ether analogues of the plant alkaloid berberine to poly(A): insights into self-structure induction, *Med. Chem. Commun*., 2011, **2**, 631-637.

10 A. Basu, P. Jaisankar and G.Suresh Kumar, 9-*O*-N-aryl/arylalkyl amino carbonyl methyl substituted berberine analogues induce self-structure in polyadenylic acid, *RSC Adv*., 2012, **2**, 7714-7723.

11 S. Taniguchi, N. Suzuki, M. Masuda, S. Hisanaga, T. Iwatsubo, M. Goedert and M. Hasegawa, Inhibition of heparin induced tau filament formation by phenothiazines, polyphenols, and porphyrins, *J. Biol. Chem*., 2005, **280**, 7614–7623.

12 K. J. Mellish, R. D. Cox, D. I. Vernon, J. Griffiths and S. B. Brown, In vitro photodynamic activity of a series of methylene blue analogues, *Photochem. Photobiol*., 2002, **75**, 392-397.

13 L. M. Moreira, J. P. Lyon, A. P. Romani, D. Severino, M. R. Rodrigues and H. P. M. de Oliveira, Phenotiazinium dyes as photosensitizers (PS) in photodynamic therapy (PDT): spectroscopic properties and photochemical mechanisms (Chapter 14), *Advanced aspects of spectroscopy*, pp. 393-422.

14 R. F. Donnelly, P. A. McCarron, M. M. Tunney and A. D. Woolfson, Potential of photodynamic therapy in treatment of fungal infections of the mouth. Design and characterization of a mucoadhesive patch containing toluidine blue O, *J. Photochem. Photobiol. B*: *Biol*., 2007, **86**, 59-69.

15 L. M. Moreira, J. P. Lyon, S. M. S. Tursi, I. Trajano, M. P. Felipe, M. S. Costa, M. R. Rodrigues, L. Codognoto and H. P.M. de Oliveira, Azure dyes as new photosensitizer prototypes to application in photodynamic therapy against *Candida spp., Spectroscopy*, 2010, **24**, 621-628.

16 M. Wainwright, M. N. Byrne and M. A. Gattrell, Phenothiazinium-based photobactericidal materials, *J. Photochem. Photobiol. B: Biol*., 2006, **84**, 227-230.

17 E. L. Kean, Rapid, sensitive spectrophotometric method for quantitative determination of sulfatides, *J. Lipid Res*., 1968, **9**, 319-327.

18 G. R. Webb, I. A. Macdonald and C. A. Williams, Ion pair extraction technique with azure A, for differentiating biles of normal subjects and patients with liver disease from patients with Crohn's disease with small bowel involvement, *Clinical Chem*., 1977, **23**, 460-463.

19 A. K. Baruia, R. Sharma and Y. S. Rajput, Detection of non-dairy fat in milk based on quantitative assay of anionic detergent using azure A dye, *Int. Dairy J*., 2012, **24**, 44-47.

20 Y. E. Zeng, H. S. Zhang and Z. H. Chen, Handbook of Organic Reagents, Chemical Industry Press, Beijing, 1989 Vol. 4, p. 793.

21 F. Culo, D. Sabolović, L. Somogyi, M. Marusić, N. Berbiguier and L. Galey, Anti-tumoral and anti-inflammatory effects of biological stains, *Agnets Actions*, 1991, **34**, 424-428.

22 R. H. Schirmer, H. Adler, M. Pickhardt and E. Mandelkow, "Lest we forget you--methylene blue...", *Neurobiol. Aging*, 2011, **32**, 2325.e7-16.

23 B. Narayana and K. Sunil, Facile and sensitive spectrophotometric method for the determination of vanadium, *Eurasian J. Anal. Chem*., 2009, **4**, 141-151.

24 M. Mathew and B. Narayana, An easy spectrophotometric determination of selenium using azure B as chromogenic reagent, *Indian J. Chem. Technol*., 2006, **13**, 455-458.

25 A. Petzer, B. H. Harvey, G. Wegener and J. P. Petzer, Azure B, a metabolite of methylene blue, is a high-potency, reversible inhibitor of monoamine oxidase, *Toxicol. Appl. Pharmacol*., 2012, **258**, 403–409.

26 P. Paul and G.Suresh Kumar, Spectroscopic studies on the binding interaction of phenothiazinium dyes toluidine blue O, azure A and azure B to DNA, *Spectrochim. Acta A*., 2013, **107**, 303-310.

27 J. D. McGhee and P. H. Von Hippel, Theoretical aspects of DNA-protein interactions: cooperative and noncooperative binding of large ligands to a one dimensional homogeneous lattice, *J. Mol. Biol*., 1974, **86**, 469-489.

28 A. Das, K. Bhadra and G.Suresh Kumar, Targeting RNA by small molecules: comparative structural and thermodynamic aspects of aristololactam-β-D-glucoside and daunomycin binding to $tRNA^{phe}$, *PLoS ONE*, 2011, **6**(**8**), e23186.

29 P. Giri and G.Suresh Kumar, Spectroscopic and calorimetric studies on the binding of the phototoxic and cytotoxic plant alkaloid sanguinarine with double helical poly(A), *J. Photochem. Photobiol. A*: *Chem*., 2008, **194**, 111-121.

30 R. Lyng, T. Hard and B. Norden, Induced CD of DNA intercalators: electric dipole allowed transitions, *Biopolymers*, 1987, **26**, 1327-1345.

31 P. Centikol and N. V. Hud, Molecular recognition of poly(A) by small ligands: an alternative method of analysis reveals nanomolar, cooperative and shape-selective binding, *Nucleic Acids Res*., 2009, **37**, 611-621.

32 P. Giri and G.Suresh Kumar, Molecular aspects of small molecules-poly(A) interaction: an approach to RNA based drug design, *Curr. Med. Chem*., 2009, **16**, 965-987.

33 M. M. Islam, S. R. Chowdhury and G.Suresh Kumar, Spectroscopic and calorimetric studies on the binding of alkaloids berberine, palmatine and coralyne to double stranded RNA polynucleotides, *J. Phys. Chem. B*, 2009, **113**, 1210-1224.

34 P. Paul, M. Hossain and G.S. Kumar, Calorimetric and thermal analysis studies on the binding of phenothiazinium dye thionine with DNA polynucleotides, *J. Chem. Thermodyn*., 2011, **43**, 1036-1043.

35 M. Hossain, P. Giri and G.Suresh Kumar, DNA intercalation by quinacrine and methylene blue: a comparative binding and thermodynamic characterization study, DNA *Cell Biol*., 2008, **27**, 81-90.

36 I. Saha, M. Hossain and G.Suresh Kumar, Sequence selective binding of phenazinium dyes, phenosafranin and safranin O to guanine-cytosine deoxyribopolynucleotides: spectroscopic and thermodynamic studies, *J. Phys. Chem. B*, 2010, **114**, 15278-15287.

37 A. Basu, P. Jaisankar and G.Suresh Kumar, Binding of the 9-O-N-aryl/arylalkyl amino carbonyl methyl substituted berberine analogs to $tRNA^{phe}$, *PLoS ONE*, 2013, **8**(**3**), e58279.

38 M. Hossain, A. Kabir and G.Suresh Kumar, Binding of the anticancer alkaloid sanguinarine with $tRNA^{phe}$: spectroscopic and calorimetric studies. *J. Biomol. Struct. Dyn*., 2012, **30**, 223-234.

39 J. Gómez and E. Freire, Thermodynamic mapping of the inhibitor site of the aspartic protease endothiapepsin, *J. Mol. Biol*., 1995, **252**, 337-350.

40 J. Ren, T. C. Jenkins and J. B. Chaires, Energetics of DNA intercalation reactions, *Biochemistry*, 2000, **39**, 8439-8447.

41 K. L. Buchmueller, S. L. Bailey, D. A. Matthews, Z. T. Taherbhai, J. K. Register, Z.S. Davis, C.D.Bruce, C.O'Hare, J.A.Hartley and M. Lee, Physical and structural basis for the strong interactions of the –ImPy-central pairing motif in the polyamide f-ImPyIm, *Biochemistry*, 2006, **45**, 13551-13565.

42 F. V. Murphy 4th and M. E. Churchill, Nonsequence-specific DNA recognition: a structural perspective, *Structure*, 2000, **8**, R83-R89.

43 J. H. Ha, R. S. Spolar and M. T. Record Jr., Role of the hydrophobic effect in stability of site specific protein-DNA complexes, *J. Mol. Biol*., 1989, **209**, 801-816.

44 K. M. Guthrie, A. D. C. Parenty, L. V. Smith, L. Cronin and A. Cooper, Microcalorimetry of interaction of dihydro-imidazo-phenanthridinium (DIP)-based compounds with duplex DNA, *Biophys. Chem*., 2007, **126**, 117-123.

45 M. M. Islam, P. Pandya, S. Kumar and G.Suresh Kumar, RNA targeting through binding os small molecules: studies on t-RNA binding by the cytotoxic protoberberine alkaloid coralyne, *Mol. Biosyst*., 2009, **5**, 244-254.

46 L. Jen-Jacobson, L. E. Engler and L. A. Jacobson, Structural and thermodynamic strategies for site-specific DNA binding proteins, *Structure*, 2000, **8**, 1015–1023.

47 E. V. Starikov and B. Norden, Enthalpy-entropy compensation: a phantom or something useful?, *J. Phys. Chem. B*, 2007, **111**, 14431–14435.

48 C. Ciatto, M. L. D'Amico, G. Natile, F. Secco and M. Venturini, Intercalation of proflavine and a platinum derivative of proflavine into double-helical poly(A), *Biophys. J.*, 1999, **77**, 2717-2724.

49 R. Nandi, D. Debnath and M. Maiti, Interactions of berberine with poly(A) and tRNA, *Biochim. Biophys. Acta*, 1990, **1049**, 339-342.

50 A. Chakraborty, M. Ali and S. K. Saha, Molecular interaction of organic dyes in bulk and confined media, *Spectrochim. Acta Part A*, 2010, **75**, 1577-1583.

51 R. Sinha, M. M. Islam, K. Bhadra, G.Suresh Kumar, A. Banerjee and M. Maiti, The binding of DNA intercalating and non-intercalating compounds to A-form and protonated form of poly(rC).poly(rG): spectroscopic and viscometric study, *Bioorg. Med. Chem*., 2006, **14**, 800-814.

52 P. Job, Formation and stability of inorganic complexes in solution, *Ann. Chim*., 1928, **9**, 113-203.

53 C. Y. Huang, S. P. Colowick, N.O. Kaplan (Eds.), Methods Enzymol, vol. 87, Academic Press, New York, 1982, pp. 509–525.

54 Z. D. Hill and M. Patrick, Novel approach to Job's method: an undergraduate experiment, *J. Chem. Educ*., 1986, **63**, 162-167.

55 A. Larsson, C. Carlsson, M. Jonsson and B. Albinsson, Characterization of the binding of the fluorescent dyes YO and YOYO to DNA by polarized light spectroscopy, *J. Am. Chem. Soc*., 1994, **116**, 8459–8465.

56 C. V. Kumar and E. H. Asuncion, Sequence dependent energy transfer from DNA to a simple aromatic chromophore, *J. Chem. Soc. Chem. Commun*., 1992, **6**, 470-472.

57 N. K. Modukuru, K. J. Snow, B.S. Perrin Jr., A. Bhambhani, M. Duff and C. V. Kumar, Tuning the DNA binding modes of an anthracene derivative with salt, *J. Photochem. Photobiol. A: Chem*., 2006, **177**, 43–54.

58 S. Das and G.Suresh Kumar, Molecular aspects on the interaction of phenosafranine to deoxyribonucleic acid: model for intercalative drug-DNA binding, *J. Mol. Struct*., 2008, **872**, 56-63.

59 M. M. Islam, R. Sinha and G.Suresh Kumar, RNA binding small molecules: studies on t-RNA binding by cytotoxic plant alkaloids berberine, palmatine and the comparison to ethidium, *Biophys. Chem*., 2007, **125**, 508-520.

60 M. M. Islam, P. Pandya, S. R. Chowdhury, S. Kumar and G.Suresh Kumar, Binding of DNA-binding alkaloids berberine and palmatine to tRNA and comparison to ethidium: spectroscopic and molecular modeling studies, *J. Mol. Struct*., 2008, **891**, 498-507.

Table 1: Binding parameters for the complexation of the dyes with ss poly(A) evaluated from Scatchard analysis of the absorbance and fluorescence titration data.

Dye	Absorbance				Fluorescence			
	$K\times10^{-5}$ $(M^{-1})^b$	n	ω	$K_i\times10^{-6}$ $(M^{-1})^b$	$K\times10^{-5}$ $(M^{-1})^b$	n	ω	$K_i\times10^{-6}$ $(M^{-1})^b$
AA	1.02	2.69	30	3.06	0.51	3.03	58	2.96
AB	1.17	3.22	14	1.65	0.72	3.11	13	0.94

[a]Average of four determinations. [b]Cooperative binding constants (K) and the number of binding sites (n) refer to solution conditions of 50 mM cacodylate buffer, pH 7.2 at 20°C. ω is the cooperativity factor. The apparent binding constants (K_i) is the product of K and the cooperative factor (ω).

Table 2: Temperature dependent isothermal titration calorimetric data for the binding of AA and AB to ss poly(A).

Dye	T (^oC)	$K_a \times 10^{-6}$ (M^{-1})	n	ΔG^o (kcal / mole)	ΔH^o (kcal / mole)	$T\Delta S^o$ (kcal/ mole)	ΔC_p^o (cal./ mole.K)	ΔG_{hyd}^o (kcal / mole)
AA	10	3.96±0.04	2.58	-8.53±0.03	-1.37±0.03	7.16	-142.23±0.04	-11.37±0.04
	15	3.17±0.03	2.81	-8.59±0.03	-2.23±0.03	6.36		
	20	2.32±0.03	2.96	-8.64±0.03	-3.01±0.03	5.63		
	30	0.97±0.03	2.99	-8.68±0.03	-4.24±0.03	4.44		
AB	10	3.08±0.03	3.01	-8.41±0.03	-1.09±0.03	7.32	-124.34±0.01	-9.95±0.01
	15	2.08±0.03	3.11	-8.46±0.03	-1.64±0.03	6.82		
	20	1.46±0.04	3.19	-8.54±0.04	-2.18±0.04	6.36		
	30	0.86±0.03	3.22	-8.56±0.03	-3.57±0.03	4.99		

[a]All the data in this table were derived from ITC experiments conducted in 50 mM cacodylate buffer, pH 7.2 and are average of four determinations. T denotes the temperatures studied. K_a, the binding affinity and ΔH^o, the standard molar enthalpy change were determined from ITC profiles fitting to Origin 7.0 software as described in the text. n, the reciprocal of N, is the site size. The values of ΔG^o, standard molar Gibbs energy change and $T\Delta S^o$, the standard molar entropy contribution were determined using the equations ΔG^o = -RT ln K_a, and $T\Delta S^o = \Delta H^o - \Delta G^o$. ΔG_{hyd}^o is the Gibbs energy contribution from the hydrophobic transfer of binding of the dyes and ΔC_p^o denotes heat capacity changes. All the ITC profiles were fit to a single binding site model. Uncertainties correspond to regression standard errors.

Table 3: ITC derived thermodynamic parameters for the binding of AA and AB to ss poly(A) at different salt concentration[a].

Dye	c (NaCl) (mM)	$K_a \times 10^{-6}$ (M^{-1})	ΔG^o (kcal/mole)	ΔH^o (kcal/mole)	$T\Delta S^o$ (kcal/mole)
AA	10	0.78±0.09	-7.95±0.09	-3.94±0.09	4.01
	50	2.32±0.05	-8.64±0.05	-3.01±0.05	5.63
	100	5.22±0.04	-9.06±0.04	-1.53±0.04	7.53
	200	7.59±0.01	-9.28±0.01	-1.45±0.01	7.83
AB	10	0.45±0.01	-7.58±0.01	-2.07±0.01	5.51
	50	1.46±0.02	-8.54±0.02	-2.18±0.02	6.36
	100	2.19±0.03	-8.59±0.01	-0.93±0.01	7.66
	200	4.25±0.02	-8.82±0.01	-0.88±0.01	7.99

[a]All the data in this table were derived from ITC experiments conducted in sodium cacodylate buffer of concentraion (c) of NaCl, 10, 20, 50, and 100 mM, pH 7.2 at 20°C and are average of four determinations. Binding constant K_a, standard molar Gibbs energy change ΔG^o, standard molar enthalpy change ΔH^o and standard molar entropic contribution $T\Delta S^o$ were derived from equations described in the legend of Fig. 2. Uncertainties correspond to regression standard errors.

FIGURE CAPTIONS

Fig. 1. Chemical structure of (a) AA and (b) AB.

Fig. 2. Absorption spectra of (a) AA (1.25 μM) treated with 0, 1.25 2.5, 5.0, 8.75, 12.5, 16.25, 18.75, 21.25, 23.75, and 26.25 μM (curves 1-11) of ss poly(A), and (b) AB (1.75 μM) treated with 0, 3.50, 7.0, 14.0, 17.5, 24.5, 28.0, 35.0 and 38.50 μM (curves 1-9) of ss poly(A). Fluorescence spectral changes of (c) AA (0.7 μM) treated with 0, 0.7, 1.4, 3.5, 5.6, 8.4, 10.5, 11.9, 13.3 and 14.7 μM (curves 1-10) of ss poly(A), and (d) AB (1.14 μM) treated with 0, 2.28, 5.6, 9.12, 11.4, 15.96, 18.24, 22.80 and 25.08 μM (curves 1-9) of ss poly(A). Inset: Representative Scatchard plot of the binding. Measurements were performed in quartz cuvettes of 1 cm path length. The excitation wavelength for AA and AB were 632 nm and 648 nm, respectively, keeping an excitation and emission band pass of 5 nm.

Fig. 3. Variation of fluorescence anisotropy as a function of [poly(A)]/[dye] for azure A (▲) and azure B (Δ). Measurements were performed in a quartz cuvette of 1 cm path length. AA and AB were excited at 632 nm and 648 nm, respectively and fluorescence signal was monitored at 645 nm and 662 nm, respectively. The excitation and emission slit widths were fixed at 5 nm.

Fig. 4. (a) Schematic energy level diagram for the energy transfer from adenine bases of poly(A) to the dyes. (b) Fluorescence excitation spectrum of AA recorded in the presence of poly(A) at emission wavelength 645 nm. (c) Sensitized fluorescence spectra of AA with (curve 1) and without (curve 2) poly(A) and (d) variation of relative quantum yield of AA (▲) and AB (Δ) in the presence of poly(A) as a function of wavelength, keeping the emission spectra fixed at 645 nm and 662 nm, respectively, for AA and AB. Excitation spectra of (e) AA (curve 1) and AA-

poly(A) complex (curve 2) keeping the emission maxima fixed at 645 nm and (f) AB (curve 1) and AB-poly(A) complex (curve 2) keeping the emission maxima fixed at 662 nm.

Fig. 5. Intrinsic circular dichroism spectra of ss poly(A) (60 μM) treated with (a) 0, 6, 12, 24, 36, 48 and 60 μM of AA (curves 1-7), and (b) 0, 6, 12, 24, 36, 48 and 60 μM of AB (curves 1-7). The expressed molar ellipticity (θ) values are based on poly(A) concentration. Measurments were performed in a rectangular quartz cuvette of 1 cm path length.

Fig. 6. Optical thermal melting profiles of (a) poly(A) (○) and poly(A)-ABcomplex (Δ) monitored at 257 nm. (b) Circular dichroism melting profiles of poly(A) (inset of Fig. 5b) and poly(A)-AAcomplex monitored at wavelength 257 nm. DSC thermogram of poly(A) (curve 1 of Fig. 6c and 6d) and (c) poly(A)-AA complex (curve 2) and (d) poly(A)-AB complex (curve 2), at 50 mM sodium cacodylate buffer.

Fig. 7. ITC profiles for the titration of (a) AA (▲) and (b) AB (Δ) with ss poly(A) at 20^{o}C in 50 mM sodium cacodylate buffer of pH 7.2. The top panels represent the raw data for the sequential injection of the dyes into ss poly(A) and the bottom panels show the integrated heat data after correction of heat of dilution against the molar ratio of ss poly(A) /dye. The data points [▲, AA-ss poly(A) and Δ, AB-ss poly(A)] reflect the experimental injection heat, which were fitted to one site model and the solid lines represent the best-fit data.

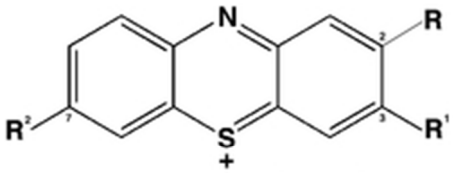

	R	R^1	R^2
(a) AA	H	NMe_2	NH_2
(b) AB	H	NMe_2	NHMe

Fig. 1

Chemical structure of (a) AA and (b) AB.
19x12mm (300 x 300 DPI)

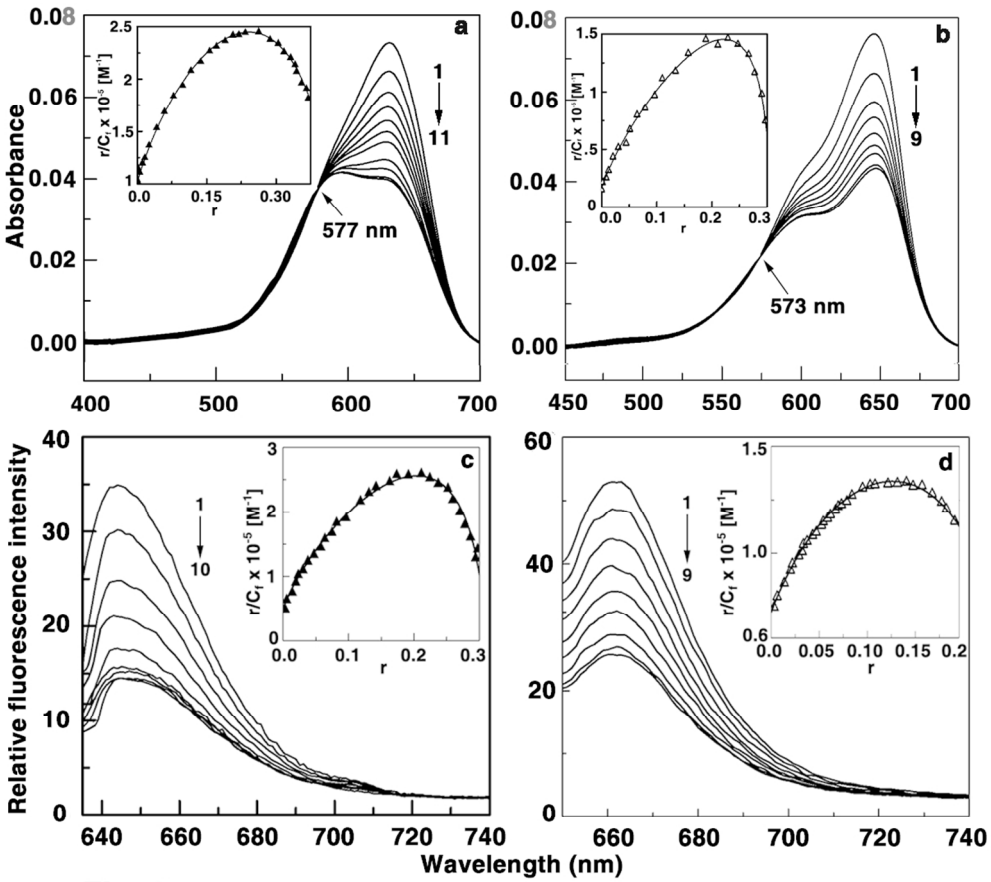

Fig. 2

Absorption spectra of (a) AA (1.25 μM) treated with 0, 1.25 2.5, 5.0, 8.75, 12.5, 16.25, 18.75, 21.25, 23.75, and 26.25 μM (curves 1-11) of ss poly(A), and (b) AB (1.75 mM) treated with 0, 3.50, 7.0, 14.0, 17.5, 24.5, 28.0, 35.0 and 38.50 mM (curves 1-9) of ss poly(A). Fluorescence spectral changes of (c) AA (0.7 mM) treated with 0, 0.7, 1.4, 3.5, 5.6, 8.4, 10.5, 11.9, 13.3 and 14.7 μM (curves 1-10) of ss poly(A), and (d) AB (1.14 μM) treated with 0, 2.28, 5.6, 9.12, 11.4, 15.96, 18.24, 22.80 and 25.08 mM (curves 1-9) of ss poly(A). Inset: Representative Scatchard plot of the binding. Measurements were performed in quartz cuvettes of 1 cm path length. The excitation wavelength for AA and AB were 632 nm and 648 nm, respectively, keeping an excitation and emission band pass of 5 nm.
103x94mm (300 x 300 DPI)

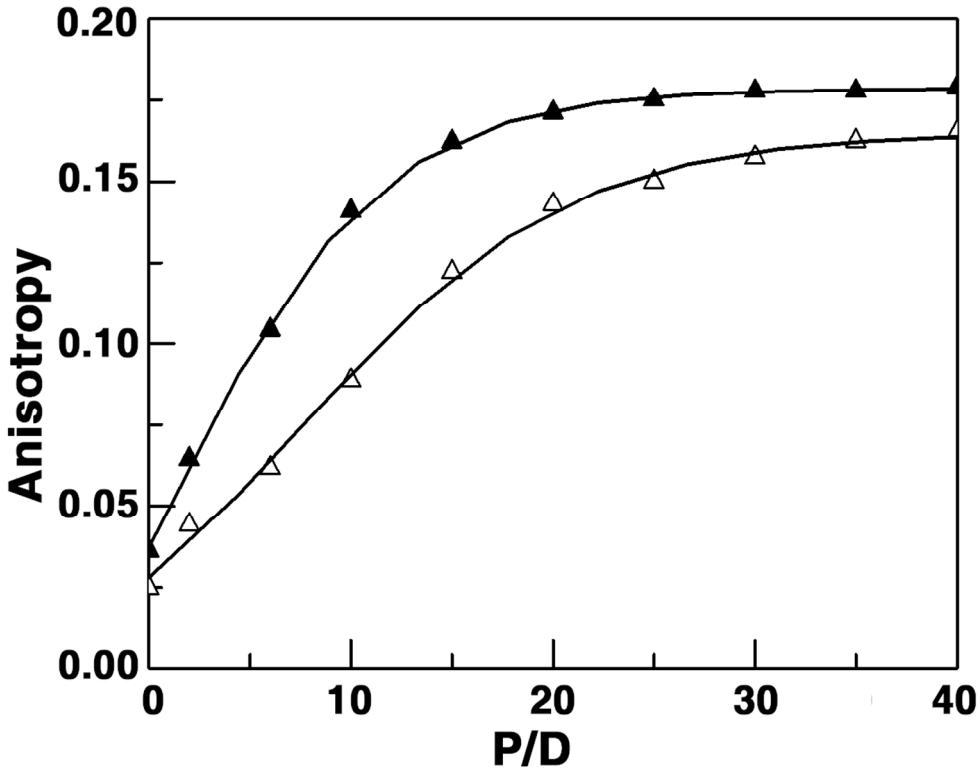

Fig. 3

Variation of fluorescence anisotropy as a function of [poly(A)]/[dye] for azure A (▲) and azure B (Δ). Measurements were performed in a quartz cuvette of 1 cm path length. AA and AB were excited at 632 nm and 648 nm, respectively and fluorescence signal was monitored at 645 nm and 662 nm, respectively. The excitation and emission slit widths were fixed at 5 nm.
107x90mm (300 x 300 DPI)

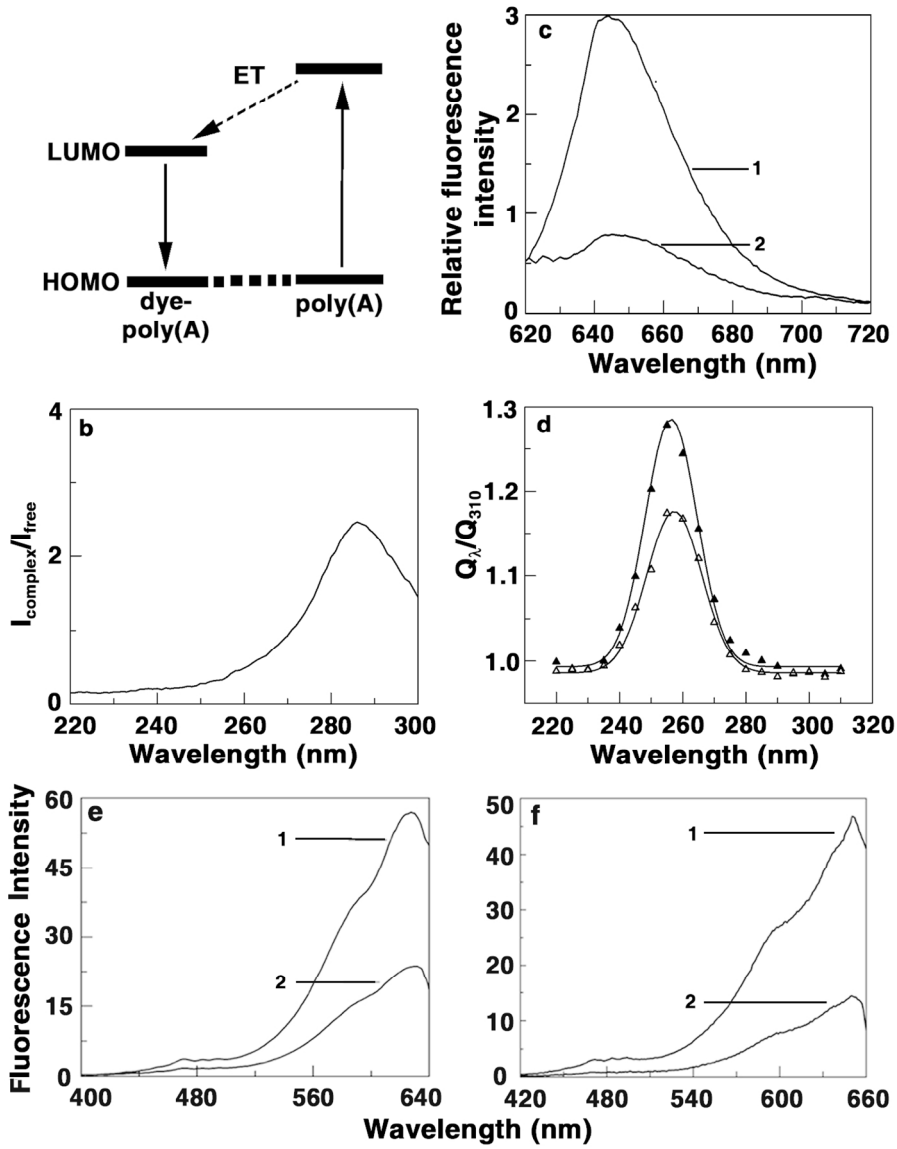

Fig. 4

Fig. 4. (a) Schematic energy level diagram for the energy transfer from adenine bases of poly(A) to the dyes. (b) Fluorescence excitation spectrum of AA recorded in the presence of poly(A) at emission wavelength 645 nm. (c) Sensitized fluorescence spectra of AA with (curve 1) and without (curve 2) poly(A) and (d) variation of relative quantum yield of AA (▲) and AB (Δ) in the presence of poly(A) as a function of wavelength, keeping the emission spectra fixed at 645 nm and 662 nm, respectively, for AA and AB. Excitation spectra of (e) AA (curve 1) and AA-poly(A) complex (curve 2) keeping the emission maxima fixed at 645 nm and (f) AB (curve 1) and AB-poly(A) complex (curve 2) keeping the emission maxima fixed at 662 nm.
118x156mm (300 x 300 DPI)

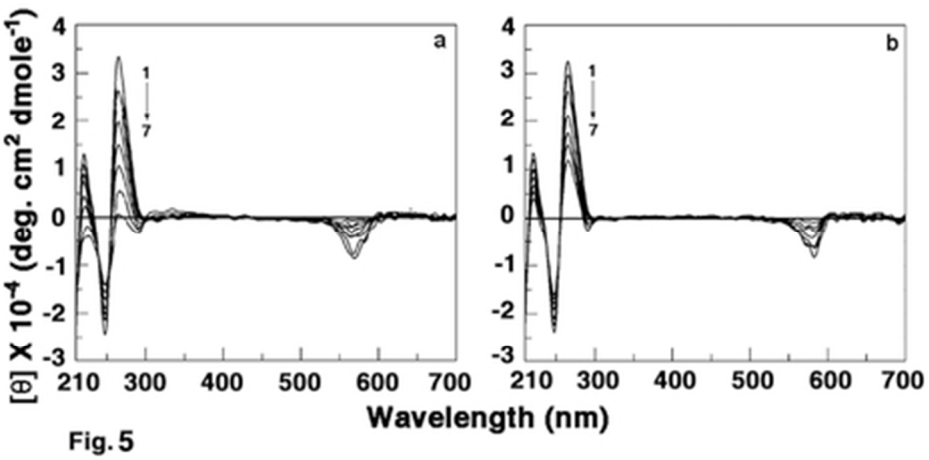

Fig. 5

Intrinsic circular dichroism spectra of ss poly(A) (60 μM) treated with (a) 0, 6, 12, 24, 36, 48 and 60 μM of AA (curves 1-7), and (b) 0, 6, 12, 24, 36, 48 and 60 μM of AB (curves 1-7). The expressed molar ellipticity (q) values are based on poly(A) concentration. Measurments were performed in a rectangular quartz cuvette of 1 cm path length.
39x19mm (300 x 300 DPI)

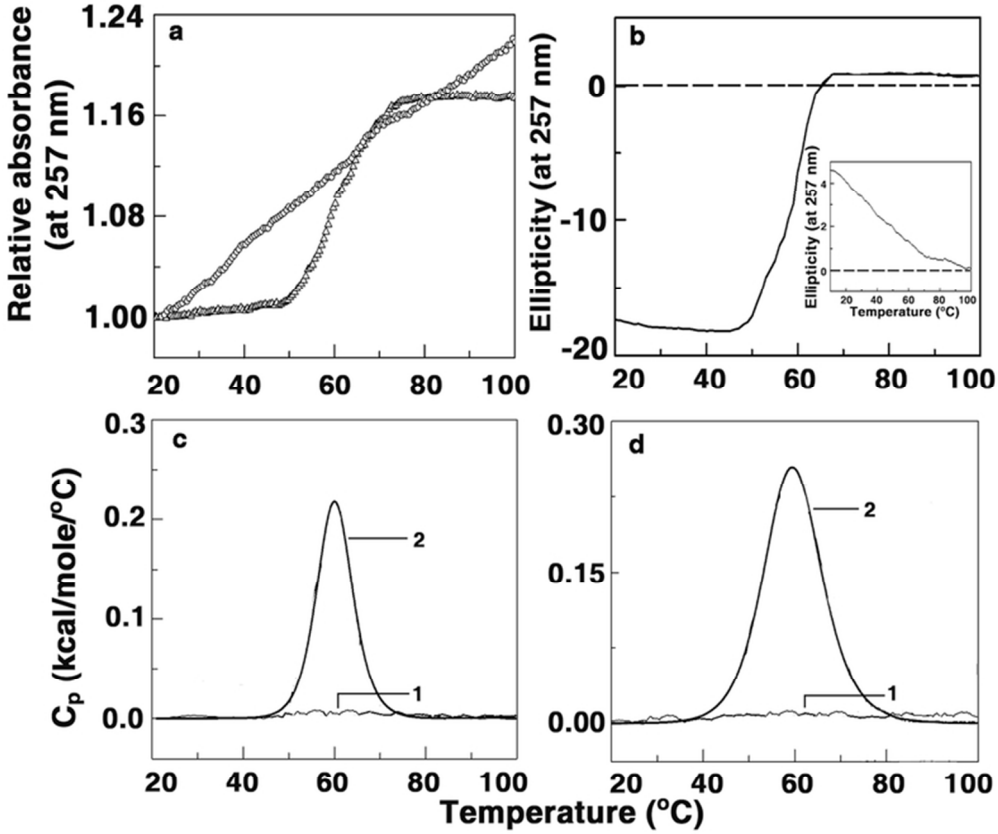

Fig.6

Optical thermal melting profiles of (a) poly(A) (○) and poly(A)-AB complex (Δ) monitored at 257 nm. (b) Circular dichroism melting profiles of poly(A) (inset of Fig. 5b) and poly(A)-AAcomplex monitored at wavelength 257 nm. DSC thermogram of poly(A) (curve 1 of Fig. 6c and 6d) and (c) poly(A)-AA complex (curve 2) and (d) poly(A)-AB complex (curve 2), at 50 mM sodium cacodylate buffer.
66x58mm (300 x 300 DPI)

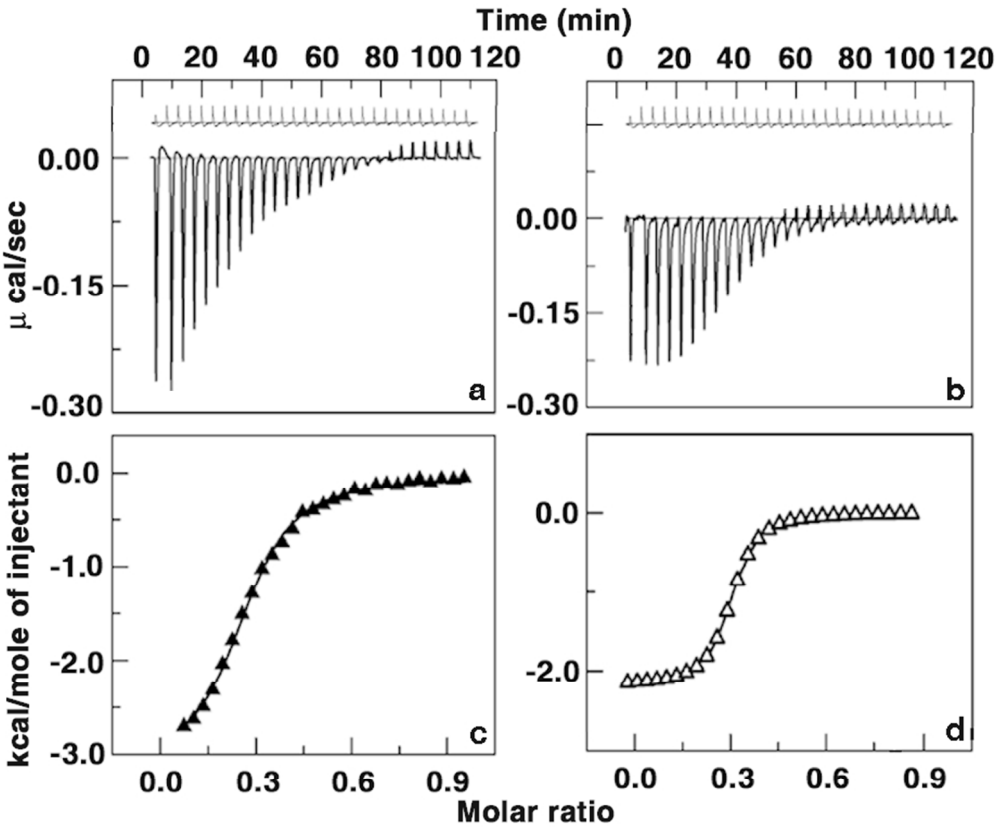

Fig. 7

ITC profiles for the titration of (a) AA (▲) and (b) AB (Δ) with ss poly(A) at 20oC in 50 mM sodium cacodylate buffer of pH 7.2. The top panels represent the raw data for the sequential injection of the dyes into ss poly(A) and the bottom panels show the integrated heat data after correction of heat of dilution against the molar ratio of ss poly(A) /dye. The data points [▲, AA-ss poly(A) and Δ, AB-ss poly(A)] reflect the experimental injection heat, which were fitted to one site model and the solid lines represent the best-fit data.
78x68mm (300 x 300 DPI)

Graphical Abstract

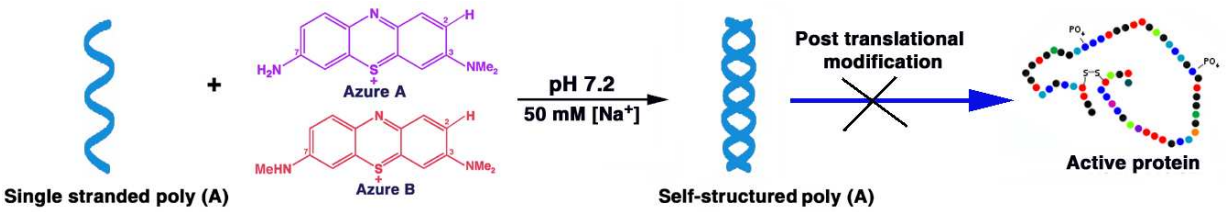

Binding of phenothaizinium dyes azure A and azure B to single stranded polyadenylic acid induces self-structure evidenced by cooperative melting in absorbance and circular dichroism experiments.